Journal of
Materials in Life Sciences

Vol. 2 No. 2 (2023)

Full Paper

Characterisation Analyses on Silver Nanoparticles Grafted Polyurethane as a Potential Material for Electroencephalography Electrodes

Fakhira Alanna Shabira[a], Dida Faadihilah Khrisna[a], Eko Supriyanto[a], Jens Haueisen[b], Syafiqah Saidin[a,c*]

[a] Department of Biomedical Engineering and Health Sciences, Faculty of Electrical Engineering Universiti Teknologi Malaysia, 81310 UTM Johor Bahru, Johor, Malaysia.
[b] Institute of Biomedical Engineering and Informatics, Technische Universität Ilmenau, Germany.
[c] IJN-UTM Cardiovascular Engineering Centre, Institute of Human Centered Engineering, Universiti Teknologi Malaysia, 81310 UTM Johor Bahru, Johor, Malaysia.

Article history
Received
25 September 2023
Revised
31 October 2023
Accepted
5 November 2023
Published online
25 November 2023

*Corresponding author
syafiqahsaidin@biomedical.utm.my

Abstract

The development of dry electrodes for electrophysiological signal detection has rapidly increased in recent years to replace the use of wet electrodes. Researchers have explored different materials and designs in developing reliable and user-friendly dry electrodes. The utilization of organic-based material such as biocompatible synthetic polymer is necessary to produce a better skin interface for electrophysiological signal detection. Therefore, this study aims to surface modify the based-substrate of polyurethane (PU) by employing polydopamine (PDA) as a mediator layer to immobilize different concentrations (25, 50 and 100 mM $AgNO_3$) of conductive silver nanoparticles (AgNPs) onto the PU surfaces. The chemical functionality and morphology analyses were performed on the samples using attenuated total reflectance-Fourier transform infrared spectroscopy (ATR-FTIR) and scanning electron microscope/energy dispersive X-ray (SEM/EDX), respectively. The wettability contact angle instrument was then used to determine the wettability properties of the samples. The ATR-FTIR analysis indicated the existence of N–H group, C–O stretch, C–H, C=O and C–N bonds which belong to the chemical functionalities of PU/PDA. While the SEM/EDX results showed that the PU/PDA/50AgNPs contained the most optimal AgNPs distribution on the PU/PDA surfaces with less particle agglomeration. Other than that, the PU/PDA/50AgNPs exhibited better hydrophobicity by increasing the water contact angle of the PU/PDA from 82.96 ± 1.37° to 92.08 ± 1.98°. Therefore, the most desired physicochemical properties for the fabrication of EEG electrodes are possessed by the PU/PDA/50AgNPs due to identical chemical functionalities, desired morphology with a homogeneous dispersion of AgNPs and greater hydrophobicity.

Keywords Electroencephalography, dry electrodes, polyurethane, silver nanoparticles, polydopamine

1.0 INTRODUCTION

Since its development in the 1920s, electroencephalography (EEG) has been applied in neuroscience research due to its ability to provide qualitative information on cerebral activity, great temporal signal resolution and able to measure time-varying electric potentials [1]. Electroencephalography has been employed as a real neuroimaging approach with more recent developments in translational and computational neuroscience [2]. Due to its ability to provide continuous, real-time brain activity data, EEG is an indispensable component of the brain-computer interface. The EEG electrodes are usually constructed of Ag/AgCl. Silver (Ag) has limited solubility, resulting in the rapid saturation and establishment of equilibrium for silver chloride (AgCl), which makes it an ideal metal for metallic skin-surface electrodes [3]. Dry electrodes and wet electrodes are two distinct categories of measuring devices. Dry electrodes are commonly used in smaller, portable weighing systems and they come in the form of a

cup, disc, or needle [4,3]. While wet electrodes are more common in multi-channel systems. Semi-dry electrodes, which require only a tiny amount of electrolyte fluid, have been developed effectively in the following years, combining the benefits of wet and dry electrodes while addressing their shortcomings in skin preparation and the usage of a wet gel [4].

Wet electrodes are the type of electrode that needs to be used along with conductive gel to reduce resistances between the electrodes and the skin during EEG measurements. However, some patients experience skin discomfort or rashes after using wet electrodes for a few hours, which has been associated to the complication of conductive gel. Besides, the signal quality of EEG recording will be significantly hampered when the conductive gel dries up [5]. On the other hand, dry EEG electrodes do not require gel application and have been designed with various shapes to fully contact the scalp which typically utilize flexible materials and probe structures that are made to pass through the hair [6]. However, the higher impedance of the electrode skin border, extra circuitry and sensitivity to movement artefacts are known as the limitations of dry electrodes [7]. Therefore, materials exploration on the development of dry electrodes is necessary to enhance the efficacy of dry electrodes. In this study, medical grade polyurethane (PU) was used as the based-substrate for the immobilization of conductive silver nanoparticles (AgNPs) as an initiation to develop EEG dry electrodes.

Nanomaterials differ from bulk materials, atoms and molecules in their specific forms and sizes, giving them extraordinary features [8]. Silver nanoparticles (AgNPs) possess a few desirable characteristics, such as good electrical conductivity, chemical stability and antibacterial capabilities [8]. Silver nanoparticles have fascinating physical features for biosensing among all metallic NPs due to their surface plasmon resonance, enhancing their responsiveness and sensitivity as optical sensors [9]. On the other hand, PU has an exceptional structure-properties relationship that endows it with desirable characteristics such as biocompatibility, biodegradability, and the ability to be chemical, mechanical, and thermal modified [10]. The utilization of PU to be used as the based-material for EEG electrodes has also been widely explored [11]. However, PU is not a conductive material that only allows its application to be the base-structure of EEG electrodes [12]. This issue might be significantly addressed by immobilizing AgNPs on PU surfaces with the assistance of a polydopamine (PDA) crosslinking layer. The catechol functional group and the primary amine group provide PDA the superior adhesion capability, effective modification sites and excellent metal coordination [13]. Furthermore, PDA supports signal conduction similar to melanin, making it suitable to be used as a mediator layer for the development of EEG electrodes [14].

2.0 EXPERIMENTAL

2.1 Materials

Polyurethane pellets were purchased from Lubrizol Corporation, Wilmington, United States. Tris (base) ($(CH_2OH)CNH_2$) was purchased from Friendemann Schmidt Chemical. The dimethylformamide (DMF), dopamine hydrochloride ($C_8H_{11}NO_2$.HCl) and silver nitrate ($AgNO_3$) were purchased from Sigma-Aldrich, Missouri, United States.

2.2 Sample Preparation

This study involves the preparation of five samples, including PU-based material (control), PU-grafted PDA (PU/PDA) and AgNPs immobilized on PU surfaces with the aid of PDA grafting (PU/PDA/*x*AgNPs; *x* = 25, 50 and 100 mM AgNPs).

2.2.1 Preparation of PU-based Material

Polyurethane-based material was made by dissolving PU pellets in DMF at 10w/v%. The solution was poured into a glass petri dish with a diameter of 5 cm and it was kept in an oven with the temperature set to 40°C for a period of four days. After that, the PU-based material that had 5 cm diameter was cut into a square sample with a dimension of 1 cm × 1 cm.

2.2.2 Polydopamine Grafting

In order to graft PDA on the PU-based material, each PU was submerged in 2 mL of dopamine solution for 24 hours. This process was carried out at room temperature and away from direct sunlight. The dopamine solution was prepared by dissolving 20 mg of dopamine hydrochloride ($C_8H_{11}NO_2$.HCl) in 10 mL of 10 mM Tris buffer. The pH of this solution was kept stable at 8.5 to provide a medium for spontaneous polymerisation [15]. For this reason, adjusting the pH of a solution can be accomplished by adding Tris buffer solution to raise the pH level or dopamine hydrochloride to reduce the pH level. Throughout this process, the solution was continuously stirred and the solution transformed from colorless to light brown color.

2.2.3 Immobilization of Silver Nanoparticles

The AgNPs immobilization was performed by submerging each PU grafted PDA for 12 hours in 3 mL aqueous solution of $AgNO_3$ at room temperature. Three different concentrations of aqueous $AgNO_3$ solutions, 25 mM, 50 mM and 100 mM, were prepared and used for the immobilization process. At 12 hours of immersion, the PU/PDA/*x*AgNPs samples were collected and rinsed in distilled water, dried and stored in a desiccator until further use.

2.3 Chemical and Morphology Analyses

2.3.1 Fourier Transform Infrared Spectroscopy (FTIR) Analysis

PerkinElmer's ATR-FTIR instrument (Frontier spectrometer, PerkinElmer, UK) was used to analyze the functional groups on each sample. The ATR-FTIR spectra of each sample were recorded between wavelengths of 500 and 4000 cm^{-1} with a resolution of 4 cm^{-1}. Then, the ATR-FTIR spectra were imported into Originlab (Origin Pro 2023, OriginLab Corporation, United States) for bond identification.

2.3.2 Scanning Electron Microscopy with Energy Dispersive X-Ray (SEM/EDX) Analysis

The morphological structure of each sample was analyzed using SEM (TM300, Hitachi, Japan). The SEM morphological observation was performed at a magnification of 3000× with an accelerating voltage of 10 kV. The chemical composition records were then conducted by EDX detector, installed in the column of SEM. All samples were sputter-coated with platinum film for 5 minutes prior to the SEM/EDX analysis. Three measurements were taken on three different spots to obtain average atomic composition percentages.

2.4 Water Contact Angle Measurements

In this study, the wettability performance of each sample was evaluated using a dynamic contact angle analyzer called VCA Optima (AST Products, Inc., Billerica, MA, USA). The PC-connected dynamic contact angle analyzer has an optical camera, syringe, needle, movable stage and solid-state lighting. Distilled water was employed in this analysis, which was injected into a syringe and placed into the contact angle slot. Before dropping the distilled water onto the sample's surface, the stage and light exposure were adjusted to improve image quality. A droplet of 2 µL was dispensed on each sample surface in triplicate across various surface areas to determine the average contact angle. The static images of the contact angle were obtained using a high-resolution camera and the final data for the contact angle were presented as mean ± SD.

3.0 RESULTS AND DISCUSSION

3.1 Sample Fabrication

The experiment started with the sample preparation process where the first sample, PU-based material which acts as the control, was cut into a square sample of 1 cm × 1 cm, as shown in Figure 1 (a). Afterwards, the PU-based materials were grafted with PDA by submerging the control sample into dopamine solution as shown in Figure 1 (b). After 24 hours, the PU color changed to light brown as the effect of dopamine oxidative polymerization. The PU/PDA/xAgNPs were then prepared at three different concentrations. As the concentration of $AgNO_3$ increased, the color of the samples transformed into a darker formation (Figure 1 (c-e).

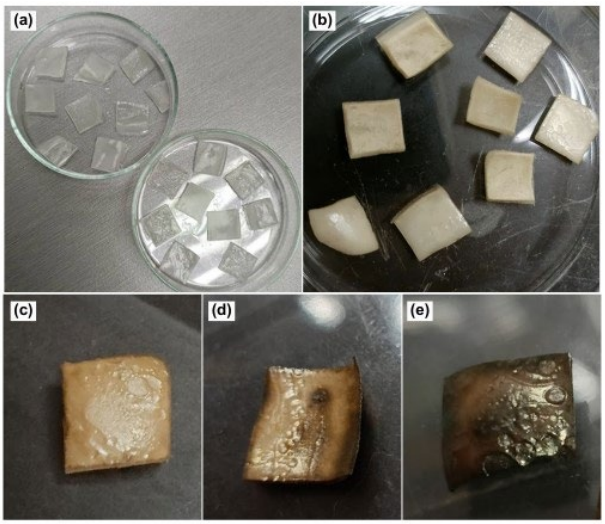

Figure 1 (a) Control, (b) PU/PDA, (c) PU/PDA/25AgNPs, (d) PU/PDA/50AgNPs and (e) PU/PDA/100AgNPs.

3.2 ATR-FTIR Analysis

Attenuated total reflectance-Fourier transform infrared can be utilized to ascertain the chemical structure of polymer materials and the presence or absence of specific functional groups. In order to identify alterations in chemical structure, the ATR-FTIR spectra were obtained within the range of 364 to 4037 cm^{-1} for various samples including PU, PU/PDA, PU/PDA/25AgNPs, PU/PDA/50AgNPs and PU/PDA/100AgNPs as presented in Figure 2.

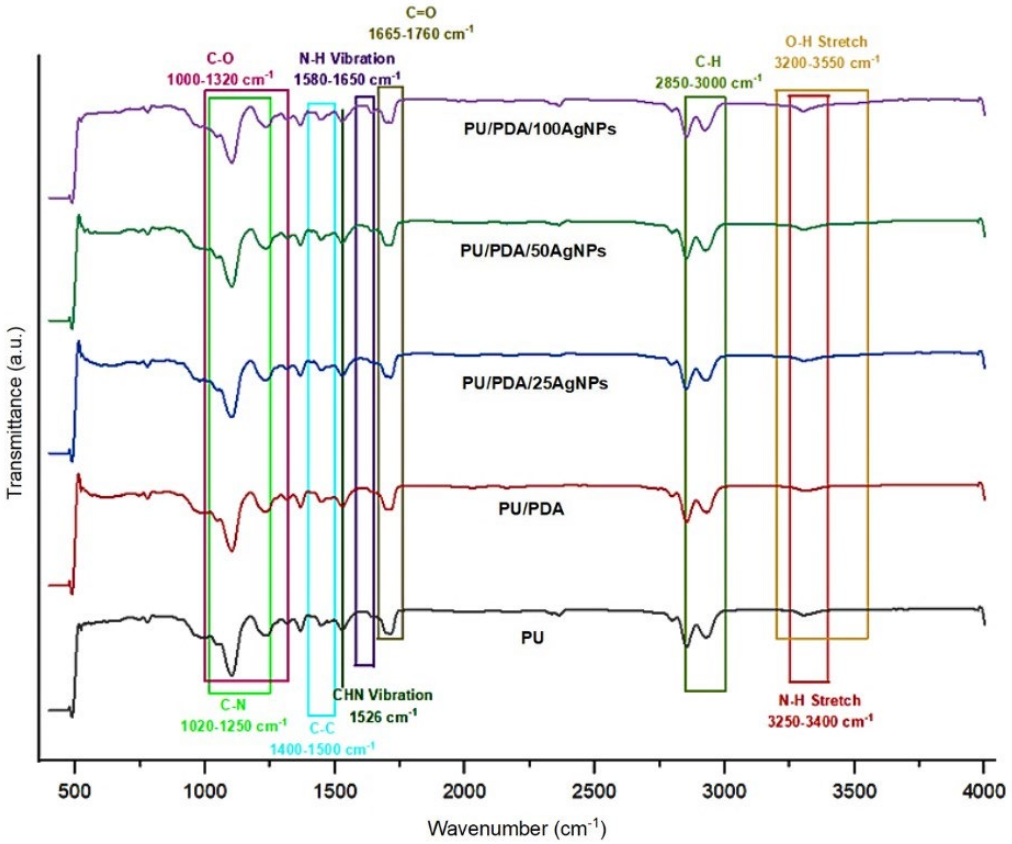

Figure 2 ATR-FTIR spectra of PU, PU/PDA, PU/PDA/25AgNPs, PU/PDA/50AgNPs and PU/PDA/100AgNPs

The absorption peak of PU is between 3250 - 3400 cm^{-1} was attributed to N–H stretching. The other peaks observed at 2850 - 3000 cm^{-1} were related to C–H stretching vibration. The absorption peak in the range of 1665 - 1760 cm^{-1} was attributed to C=O bonds. Additional peaks were detected at approximately 1526cm^{-1}, 1020 - 1250 cm^{-1} and 1000 - 1320 cm^{-1}, which corresponded to the vibrational modes of CHN, C–N and C–O stretching, respectively. The ATR-FTIR spectra of PU and PU/PDA exhibited a high degree of similarity, owing to the presence of PU as the primary constituent in both samples.

Polydopamine, a synthetic polymer that originates from dopamine, can be utilized to introduce supplementary functional groups, such as hydroxyl (O–H) and amine (-NH_2) groups, on the PU. Most functional groups of PDA were already presented in the PU backbone itself. Consequently, the existence of PDA may not induce significant alterations or modifications in the characteristic absorption bands of PU as observed in the ATR-FTIR spectra. The ATR-FTIR spectra of PU/PDA sample revealed the existence of wide peaks within 3200 - 3550 cm^{-1} and 3250 - 3400 cm^{-1} ranges, which were associated with O–H and -NH_2 of PDA. The spectral peaks detected within the range of 1580 - 1650 cm^{-1} were suggestive of the presence of an aromatic ring and N–H vibration.

Furthermore, it has been observed that Ag ions could bind with proteins and water-soluble compounds through the utilization of (O–H) and (-COOH) groups. These binding processes led to a change in the conformation of PDA molecules, which ultimately resulted in the conversion of captured metal ions into AgNPs [16]. Furthermore, PDA's inherent reductive ability enabled *in-situ* deposition of metallic Ag upon exposure to $AgNO_3$ solution [17], making the PDA layer on the PU surfaces, a useful active platform to immobilize AgNPs. In addition, the presence of amines in PDA acted as capping agents, hence promoting the immobilization of AgNPs on the PDA surfaces [18].

The analysis of the ATR-FTIR spectra for the PU/PDA/*x*AgNPS indicates the presence of a band at 1637 cm^{-1}, which originated from N–H bending mode in the amine group. Furthermore, the absorption peaks between 1000 - 1320 cm^{-1}, 1400 - 1500 cm^{-1}, 1580 - 1650 cm^{-1}, 2850 - 3000 cm^{-1}, 3250 - 3400 cm^{-1} and 3200 - 3550 cm^{-1} were attributed to C–O, C–C, N–H bending, C–H, N–H stretching and O–H stretching, respectively. The presence of AgNPs on the PDA layer was further analyzed using the SEM/EDX instrument.

3.3 SEM Analysis

In this study, SEM analysis is a necessary analysis for the proposed EEG materials since the surface features of the material can affect the electrode's performance, stability and biocompatibility. The PU backbone is composed of (-NH-COO-) urethane linkages, which consist of a hard segment composed of diisocyanates and a soft segment composed of polyols that alternate in flexibility [19]. Soft segments can possess a foundation of either polyester or polyether and exhibit unique characteristics such as hydrophilicity or hydrophobicity [19]. The SEM analysis of PU samples revealed the presence of heterogeneous morphology. The observed crystalline structure and irregularity in the SEM results may be attributed to the influence of hard and soft segments

on microphase separation [16]. The application of PDA onto the PU surfaces resulted in the improvement of surface smoothness compared to the control PU sample. The scattered small white dots that began to cluster and grew more visible in Figure 3 (c), (d) and (e) are denoted as AgNPs. These findings are further corroborated by the elemental mapping data obtained from the EDX analysis, as depicted in Figure 4. The EDX results will provide insights into the distribution of AgNPs on the PU/PDA/xAgNPs samples, hence aiding in the understanding of their dispersion.

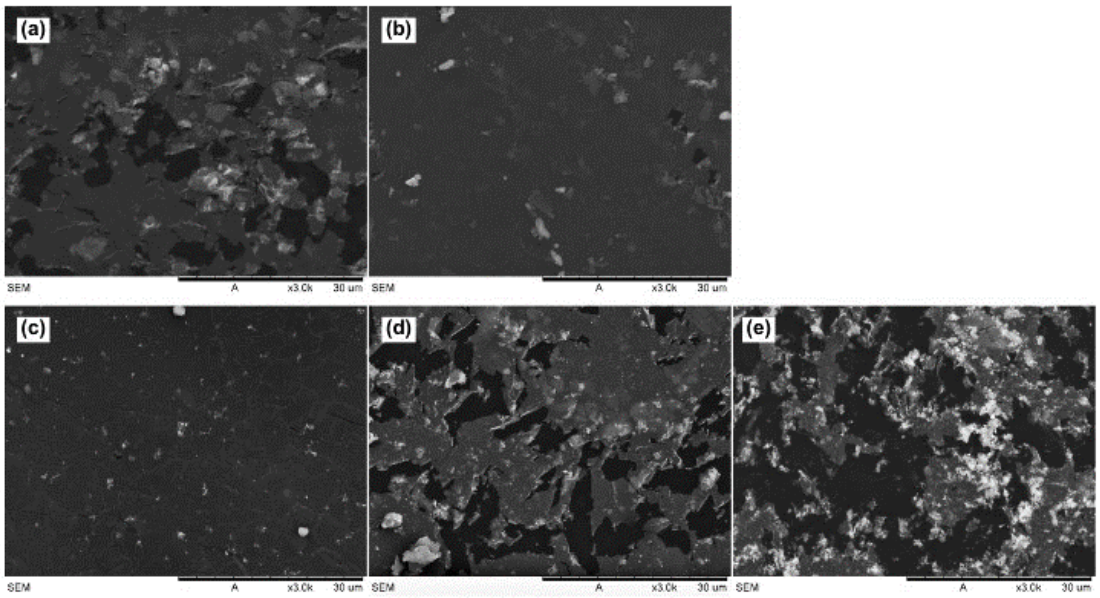

Figure 3 SEM images of (a) PU, (b) PU/PDA, (c) PU/PDA/25AgNPs, (d) PU/PDA/50AgNPs and (e) PU/PDA/100AgNPs.

The presence of catechol groups in the PDA enhanced its adhesion properties by undergoing oxidation to generate o-quinone functionalities [20]. This phenomenon is widely acknowledged as the underlying mechanism responsible for the adhesive behaviour of PDA, enabling it to adhere to a diverse range of surfaces. The surface morphology of the sample undergoes a modification after the PDA grafting process, resulting in the emergence of spherocylindrical particles, as shown in Figure 3 (b). The presence of white patches on the sample can be attributed to the agglomeration of PDA nanoparticles [21]. Efforts were made to restrict the exposure of UV to the samples undergoing immobilization by storing them at room temperature, in a location that was shielded from direct sunlight [17]. Nevertheless, there exist numerous potential factors that contributed to the clustering of PDA, necessitating additional investigation.

The PDA layers contained catechol groups that exhibited the capability to perform the reduction of metal ions, including Ag^{+}ions, by means of the metal-catechol chelation process through charge transfer. This process led to the formation of zero-valent Ag^{0} AgNPs *in-situ* [16]. In addition, the ligands present on the PDA that are based on oxygen and nitrogen acted as binding sites for the AgNPs, resulting in the formation of secondary hierarchical structures. These structures then contributed to the development of AgNPs that were composed of multiple levels of hierarchical organisation [16].

According to Figure 3 (b) and (c), there is an increase in the amount of AgNPs on the surface, as indicated by the increase in white dots, which became more visible in Figure 3 (c). At lower concentrations, AgNPs were evenly distributed across the PU/PDA surface. As the concentration of AgNPs increased, the probability of particle aggregation also increased. The presence of aggregated AgNPs can lead to the development of surface irregularities, thereby increasing the roughness and texture of the surface. The uneven layer created by the AgNPs led to the formation of uneven surfaces, which can impact its hydrophobicity. The investigation of hydrophobicity will be extended through the utilization of contact angle analysis.

3.4 EDX Analysis

The EDX was utilized to further characterize the composition of PU, PU/PDA and PU/PDA/*x*AgNPs at varying concentrations, as shown in Table 1. The EDX data of the control and PU/PDA, exhibited peaks corresponding to the elements of carbon (C), nitrogen (N) and oxygen (O). Based on the EDX results, there are significant increments in C element from 49.93 ± 0.36% to 57.30 ± 5.46% and the decrement of N element from 32.26 ± 0.68% to 22.12 ± 5.77% following the grafting of PDA on the PU surfaces. This PDA coating dominated the top sample surfaces, with high C concentration but low N content [22]. Meanwhile, the EDX results show that the PDA modification may significantly increase the surface O element concentration on the PU, from 17.81 ± 0.33% to 20.58 ± 0.32%.

As previously stated, three different concentrations of $AgNO_3$ solution were employed in this study to further evaluate the variation of AgNPs in each sample. The appearances of Ag peak and distribution indicate that the Ag particles were successfully immobilized on the surface of the PU/PDA. The surface of PDA exhibited an enrichment of catechol and amine groups, which facilitated the facile adsorption of introduced Ag precursor ions onto the PDA surface, developing AgNPs nucleation [23]. Evidently, there is a significant increment on Ag element from 0.21 ± 0.03% to 0.87 ± 0.08% when increasing the concentrations of $AgNO_3$ solution from 25 mM to 50 mM. This phenomenon is justifiable as the utilization of elevated concentrations of $AgNO_3$ solutions is likely to stimulate a greater deposition of Ag onto the PDA layer. However, the Ag element

decreased to 0.46 ± 0.12% after immobilizing the PU/PDA sample with 100 mM of $AgNO_3$ solution. As the concentration was increased, the rate of reduction correspondingly escalated, leading to a rise in the growth rate of crystals on the primary nuclei. This phenomenon impeded additional nucleation, causing smaller particles to disintegrate and adhere to the larger particles [24].

Table 1 Chemical composition obtained from EDX results.

Sample	Atomic percentage (%)			
	C	N	O	Ag
PU	49.93 ± 0.36	32.26 ± 0.68	17.81 ± 0.33	-
PU/PDA	57.30 ± 5.46	22.12 ± 5.77	20.58 ± 0.32	-
PU/PDA/25AgNPs	68.92 ± 0.26	30.86 ± 0.23	-	0.21 ± 0.03
PU/PDA/50AgNPs	66.99 ± 0.82	32.14 ± 0.75	-	0.87 ± 0.08
PU/PDA/100AgNPs	69.19 ± 1.38	30.34 ± 1.33	-	0.46 ± 0.12

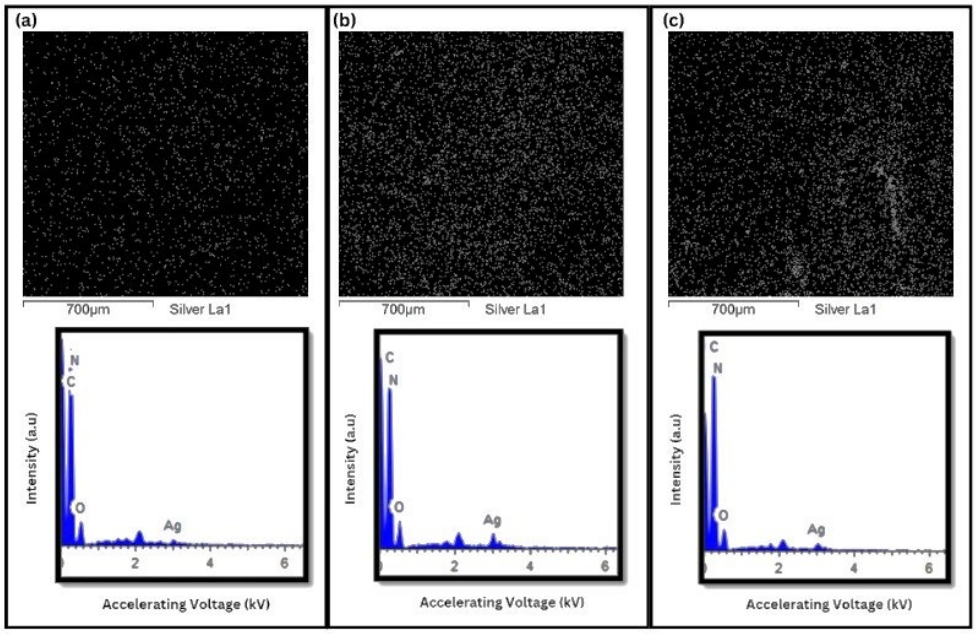

Figure 4 EDX elemental mapping of AgNPs results: (a) PU/PDA/25AgNPs, (b) PU/PDA/50AgNPs and (c) PU/PDA/100AgNPs.

3.5 Water Contact Angle Measurement

Electrode corrosion is a prevalent occurrence in metals, often resulting from the accumulation of sweat ions [25]. Sweat can compromise the EEG recording process, particularly during prolonged recording periods [25,26]. The analysis indicates that polymers are chemically stable in wet environments, while certain metals are susceptible to corrosion [27,28]. The water contact angle analysis was performed to quantify the degree of hydrophobicity exhibited by each sample. After performing the water contact angle analysis, there are three possible outcomes which are hydrophilic, hydrophobic and superhydrophobic. The hydrophilic has a behavior where it is attracted to water with a contact angle ranging between $0° < \theta < 90°$ [29]. On the other hand, hydrophobic and superhydrophobic behavior tend to repel water with the measurements of $90° < \theta < 150°$ and $\theta < 150°$, respectively [29]. Although this study does not involve bacterial analysis, it is noteworthy that hydrophobic materials can impede bacterial adherence on EEG electrodes [30].

Polyurethane is normally hydrophobic despite the surface roughness with the theoretical contact angle $\theta > 90°$ [31]. In contrast with the PU, PDA has hydroxyl and amino groups in the molecules which makes it more hydrophilic [32]. Figure 5 shows the graph for the water contact angle performed on each sample. The data obtained from the water contact angle measurement on the control samples indicate that the hydrophobicity of PU was influenced by the application of PDA coating. Initially, the analysis showed that the PU was hydrophobic with an average of 109.96 ± 0.81°. After the PU had been grafted with PDA, the sample became hydrophilic with an average contact angle of 82.96 ± 1.37°. The PDA layer has influenced the wettability behavior of PU due to the aromatic and quinone structures formed during the oxidation process that caused the PU to be more hydrophilic [21].

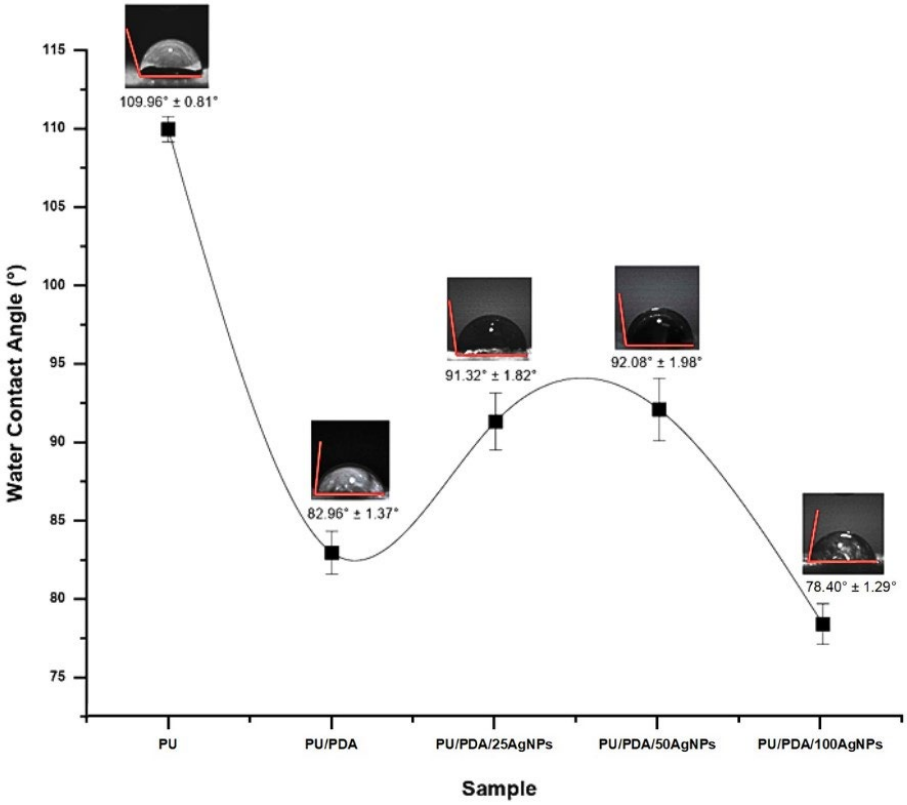

Figure 5 Water contact angle analysis.

Based on Figure 5, the contact angle values of PU/PDA increased from 82.96 ± 1.37° to 91.32 ± 1.82° and 92.08 ± 1.98° after the Ag immobilization with 25 mM and 50 mM of aqueous $AgNO_3$, respectively. The increment of hydrophobicity of PU/PDA following the Ag immobilization indicates that AgNPs have covered the PU/PDA surfaces by creating another fragmented layer above it which acted as a barrier that influenced the surface hydrophobicity. Other than that, the increase in contact angle is partially due to the incorporation of Ag ions, which have been demonstrated to yield a surface hydrophobic in nature [33]. However, the overloading of AgNPs after increasing the $AgNO_3$ concentration to 100 mM, resulted in non-uniform deposition/agglomeration of AgNPs [34]. These findings are in line with prior literature that suggests the placement of AgNPs within a matrix has the ability to alter its hydrophilicity [34].

4.0 CONCLUSION

This research explores the potential use of PU materials immobilized with AgNPs for the development of EEG electrodes. The PU surface was successfully immobilized with AgNPs using PDA, as confirmed by physicochemical and morphological analysis. However, the most effective Ag immobilization is demonstrated on the samples that were immobilized with 50 mM $AgNO_3$. In this process, the AgNPs can evenly cover the surface of PU/PDA with less agglomeration formation. The hydrophobicity of PU/PDA/50AgNPs is crucial in preventing the buildup of sweat on EEG electrodes. However, determining the best material for EEG electrodes involves more than just analyzing their physicochemical properties, morphology and wettability. Therefore, future research should prioritize the analysis of the conductivity, biocompatibility and durability of PU/PDA/50AgNPs.

Acknowledgement

The authors would like to acknowledge Universiti Teknologi Malaysia (UTM), Ministry of Education Malaysia for financial support under Research University Grant Tier 1 (Vot No: 08H01) and Faculty Bioscience and Medical Engineering (FBME).

References

[1] Chen, C. S., Chien, T. S., Lee, P. L., Jeng, Y., & Yeh, T. K. (2020). Prefrontal brain electrical activity and cognitive load analysis using a non-linear and non-stationary approach. IEEE Access, 8, 211115–211124. https://doi.org/10.1109/ACCESS.2020.3038807

[2] Biasiucci, A., Franceschiello, B., & Murray, M. M. (2019). Electroencephalography. Current Biology, 29(3), R80–R85. Cell Press. https://doi.org/10.1016/j.cub.2018.11.052

[3] Di Flumeri, G., Aricò, P., Borghini, G., Sciaraffa, N., Di Florio, A., & Babiloni, F. (2019). The dry revolution: Evaluation of three different eeg dry electrode types in terms of signal spectral features, mental states classification and usability. Sensors (Switzerland), 19(6). https://doi.org/10.3390/s19061365

[4] Barsy, B. G., Gyori, G., & Szemes, P. T. (2020). Development of EEG measurement and processing system in LabVIEW development environment. International Review of Applied Sciences and Engineering, 11(3), 287–297. https://doi.org/10.1556/1848.2020.00151

[5] Hsieh, J. C., Li, Y., Wang, H., Perz, M., Tang, Q., Tang, K. W. K., Pyatnitskiy, I., Reyes, R., Ding, H., & Wang, H. (2022). Design of hydrogel-based wearable EEG electrodes for medical applications. Journal of Materials Chemistry B, 10(37), 7260–7280. https://doi.org/10.1039/d2tb00618a

[6] Hua, H., Tang, W., Xu, X., Feng, D. D., & Shu, L. (2019). Flexible multi-layer semi-dry electrode for scalp EEG measurements at hairy sites. Micromachines, 10(8). https://doi.org/10.3390/mi10080518

[7] Tseghai, G. B., Malengier, B., Fante, K. A., & Van Langenhove, L. (2020). The status of textile-based dry eeg electrodes. Autex Research Journal. https://doi.org/10.2478/aut-2019-0071

[8] Liao, C., Li, Y., & Tjong, S. C. (2019). Bactericidal and cytotoxic properties of silver nanoparticles. International Journal of Molecular Sciences, 20(2). https://doi.org/10.3390/ijms20020449

[9] Li, Y., Li, C., Yu, R., & Ding, Y. (2022). Application of polydopamine on the implant surface modification. Polymer Bulletin, 79(8), 5613–5633. https://doi.org/10.1007/s00289-021-03793-9

[10] Naureen, B., Haseeb, A. S. M. A., Basirun, W. J., & Muhamad, F. (2021). Recent advances in tissue engineering scaffolds based on polyurethane and modified polyurethane. Materials Science and Engineering C, 118, 111228. https://doi.org/10.1016/j.msec.2020.111228

[11] He, G., Dong, X., & Qi, M. (2020). From the perspective of material science: a review of flexible electrodes for brain-computer interface. Materials Research Express, 7(10), 102001. https://doi.org/10.1088/2053-1591/abb857

[12] Matinha-Cardoso, J., Mota, R., Gomes, L. C., Gomes, M., Mergulhão, F. J., Tamagnini, P., L. Martins, M. C., & Costa, F. (2021). Surface activation of medical grade polyurethane for the covalent immobilization of an anti-adhesive biopolymeric coating. Journal of Materials Chemistry B, 9(17), 3705-3715. https://doi.org/10.1039/D1TB00278C

[13] Chen, J., Wang, Q., Luan, M., Mo, J., Yan, Y., & Li, X. (2019). Polydopamine as reinforcement in the coating of nano-silver on polyurethane surface: Performance and mechanisms. Progress in Organic Coatings, 137, 105288. https://doi.org/10.1016/j.porgcoat.2019.105288

[14] Bettucci, O., Matrone, G. M., & Santoro, F. (2022). Conductive polymer-based bioelectronic platforms toward sustainable and biointegrated devices: a journey from skin to brain across human body interfaces. Advanced Materials Technologies, 7(2), 2100293. https://doi.org/10.1002/admt.202100293

[15] Saidin, S. (2014). Immobilisation of Biomimetic Hydroxyapatite & Silver Nanoparticles. LAP LAMBERT Academic Publisher, 1, 33–35.

[16] Chew, N. G. P., Zhang, Y., Goh, K., Ho, J. S., Xu, R., & Wang, R. (2019). Hierarchically structured janus membrane surfaces for enhanced membrane distillation performance. ACS Applied Materials and Interfaces, 11(28), 25524–25534. https://doi.org/10.1021/acsami.9b05967

[17] Yassin, M. A., Elkhooly, T. A., Elsherbiny, S. M., Reicha, F. M., & Shokeir, A. A. (2019). Facile coating of urinary catheter with bio–inspired antibacterial coating. Heliyon, 5(12), e02986. https://doi.org/10.1016/j.heliyon.2019.e02986

[18] Mikhailova, E. O. (2020). Silver nanoparticles: Mechanism of action and probable bio-application. Journal of functional biomaterials, 11(4), 84. MDPI. https://doi.org/10.3390/jfb11040084

[19] Turan, D. (2021). Water Vapor Transport Properties of Polyurethane Films for Packaging of Respiring Foods. Food Engineering Reviews, 13(1), 54–65. https://doi.org/10.1007/s12393-019-09205-z

[20] Vona, D., Cicco, S. R., Ragni, R., Leone, G., Lo Presti, M., & Farinola, G. M. (2018). Biosilica/polydopamine/silver nanoparticles composites: New hybrid multifunctional heterostructures obtained by chemical modification of Thalassiosira weissflogii silica shells. MRS Communications, 8(3), 911–917. https://doi.org/10.1557/mrc.2018.103

[21] Wang, Z., Yang, H. C., He, F., Peng, S., Li, Y., Shao, L., & Darling, S. B. (2019). Mussel-inspired surface engineering for water-remediation materials. Matter, 1(1), 115-155. https://doi.org/10.1016/j.matt.2019.05.002

[22] Zhang, Y., Zeng, Z., Ma, X. Y. D., Zhao, C., Ang, J. M., Ng, B. F., Wan, M. P., Wong, S. C., Wang, Z., & Lu, X. (2019). Mussel-inspired approach to cross-linked functional 3D nanofibrous aerogels for energy-efficient filtration of ultrafine airborne particles. Applied Surface Science, 479, 700–708. https://doi.org/10.1016/j.apsusc.2019.02.173

[23] Nie, Y., Wang, T., Wu, M., Wang, C., Wang, J., & Han, Z. (2023). Enhanced bioactivity and antimicrobial properties of α-tricalcium phosphate cement via PDA@Ag coating. Materials Letters, 330. https://doi.org/10.1016/j.matlet.2022.133230

[24] Ahmad, N., Ang, B. C., Amalina, M. A., & Bong, C. W. (2018). Influence of precursor concentration and temperature on the formation of nanosilver in chemical reduction method. Sains Malaysiana, 47(1), 157–168. https://doi.org/10.17576/jsm-2018-4701-19

[25] Das, A., & Mahanwar, P. (2020). A brief discussion on advances in polyurethane applications. Advanced Industrial and Engineering Polymer Research, 3(3), 93-101. https://doi.org/10.1016/j.aiepr.2020.07.002

[26] Pajusco, P., Malhouroux-Gaffet, N., & El Zein, G. (2015). Comprehensive characterization of the double directional UWB residential indoor channel. IEEE Transactions on Antennas and Propagation, 63(3), 1129–1139. https://doi.org/10.1109/TAP.2014.2387418

[27] Chamas, A., Moon, H., Zheng, J., Qiu, Y., Tabassum, T., Jang, J. H., Abu-Omar, M., Scott, S. L., & Suh, S. (2020). Degradation rates of plastics in the environment. ACS Sustainable Chemistry and Engineering, 8(9), 3494–3511. https://doi.org/10.1021/acssuschemeng.9b06635

[28] Sazali, N., Ibrahim, H., Jamaludin, A. S., Mohamed, M. A., Salleh, W. N. W., & Abidin, M. N. Z. (2020). Degradation and stability of polymer: A mini review. IOP Conference Series: Materials Science and Engineering, 788(1), 012048. https://doi.org/10.1088/1757-899X/788/1/012048

[29] Jasmee, S., Omar, G., Masripan, N. A. B., Kamarolzaman, A. A., Ashikin, A. S., & Che Ani, F. (2018). Hydrophobicity performance of polyethylene terephthalate (PET) and thermoplastic polyurethane (TPU) with thermal effect. Materials Research Express, 5(9), 096304. https://doi.org/10.1088/2053-1591/aad81e

[30] Yang, K., Shi, J., Wang, L., Chen, Y., Liang, C., Yang, L., & Wang, L. N. (2022). Bacterial anti-adhesion surface design: Surface patterning, roughness and wettability: A review. Journal of Materials Science & Technology, 99, 82-100. https://doi.org/10.1016/j.jmst.2021.05.028

[31] Segan, S., Jakobi, M., Khokhani, P., Klimosch, S., Billing, F., Schneider, M., Martin, D., Metzger, U., Biesemeier, A., Xiong, X., Mukherjee, A., Steuer, H., Keller, B. M., Joos, T., Schmolz, M., Rothbauer, U., Hartmann, H., Burkhardt, C., Lorenz, G., Shipp, C. (2020). Systematic investigation of polyurethane biomaterial surface roughness on human immune responses in vitro. BioMed Research International, 2020. https://doi.org/10.1155/2020/3481549

[32] Xi, Z. Y., Xu, Y. Y., Zhu, L. P., Wang, Y., & Zhu, B. K. (2009). A facile method of surface modification for hydrophobic polymer membranes based on the adhesive behavior of poly(DOPA) and poly(dopamine). Journal of Membrane Science, 327(1–2), 244–253. https://doi.org/10.1016/j.memsci.2008.11.037

[33] Kraśniewska, K., Galus, S., & Gniewosz, M. (2020). Biopolymers-based materials containing silver nanoparticles as active packaging for food applications–a review. International Journal of Molecular Sciences, 21(3), 698. https://doi.org/10.3390/ijms21030698

[34] Saraswathi, M. S. S. A., Rana, D., Alwarappan, S., Gowrishankar, S., Vijayakumar, P., & Nagendran, A. (2019). Polydopamine layered poly (ether imide) ultrafiltration membranes tailored with silver nanoparticles designed for better permeability, selectivity and antifouling. Journal of Industrial and Engineering Chemistry, 76, 141–149. https://doi.org/10.1016/j.jiec.2019.03.014